1-1-2005

Analytical and numerical solutions for soft clay consolidation using geosynthetic vertical drains with special reference to embankments

Buddhima Indraratna
University of Wollongong, indra@uow.edu.au

Cholachat Rujikiatkamjorn
University of Wollongong, cholacha@uow.edu.au

Iyathurai Sathananthan
University of Wollongong

Mohamed A. Shahin
University of Wollongong, shahin@uow.edu.au

Hadi Khabbaz
University of Wollongong, khabbaz@uow.edu.au

ANALYTICAL AND NUMERICAL SOLUTIONS FOR SOFT CLAY CONSOLIDATION USING GEOSYNTHETIC VERTICAL DRAINS WITH SPECIAL REFERENCE TO EMBANKMENTS

Buddhima Indraratna

PhD, DIC, MSc (Lond.), FIEAust., FASCE

Professor of Civil Engineering, Faculty of Engineering,

University of Wollongong, Wollongong City, NSW 2522, Australia

Tel: +61-2-4221-3046; Fax: +61-2-4221-3238

E-mail: indra@uow.edu.au

Cholachat Rujikiatkamjorn

BEng (Hons), MEng (AIT), MIEAust

Doctoral Student, Civil Engineering, Faculty of Engineering,

University of Wollongong, Wollongong City, NSW 2522, Australia

Iyathurai Sathananthan

BEng (Hons)

Doctoral Student, Civil Engineering, Faculty of Engineering

University of Wollongong, Wollongong City, NSW 2522, Australia

Mohamed A. Shahin

BSc, MSc, PhD, MIEAust

Research Fellow, Civil Engineering, Faculty of Engineering

University of Wollongong, Wollongong City, NSW 2522, Australia

Hadi Khabbaz

BSc, MSc, PhD

Research Fellow, Civil Engineering, Faculty of Engineering

University of Wollongong, Wollongong City, NSW 2522, Australia

The Fifth International Geotechnical Engineering Conference, Cairo

ANALYTICAL AND NUMERICAL SOLUTIONS FOR SOFT CLAY CONSOLIDATION USING GEOSYNTHETIC VERTICAL DRAINS WITH SPECIAL REFERENCE TO EMBANKMENTS

Buddhima Indraratna[1†], Cholachat Rujikiatkamjorn[2], Iyathurai Sathananthan[2], Mohamed A. Shahin[3] and Hadi Khabbaz[3]

ABSTRACT

Good quality geologic materials for construction are also becoming scarce. Due to these reasons and because of the environmental restrictions on certain public works, ground improvement is becoming an essential part of infrastructure development. As a result, Civil Engineers are forced to utilise even the poorest soft clay foundations for buildings, highways and railway tracks. Therefore, the application of prefabricated vertical drains with preloading has now become common practice and one of the most effective ground improvement techniques. The classical solution for vertical drains (single drain analysis) has been well documented in the literature, where there are many vertical drains, a true 3-D analysis of the site becomes very difficult. Therefore, equivalent 2-D plane strain models have been employed, using the methods of geometric and permeability matching concepts. The equivalent plane strain solution can now be used as a predictive tool with acceptable accuracy as a result of the significant process that has been made in the past few years through rigorous mathematical modelling and numerical analyses.

In this paper, the equivalent 2-D plane strain solution is described which includes the effects of smear zone caused by mandrel driven vertical drains. The equivalent (transformed) permeability coefficients are incorporated in finite element codes, employing the modified Cam-clay theory. Numerical analysis is conducted to predict the excess pore pressures, lateral and vertical displacements. Two case histories are discussed and analysed, including the sites of Muar clay (Malaysia) and the predictions are compared with the available field data. The research findings verify that the impact of smear and well resistance can significantly affect soil consolidation, hence, in order to obtain reliable consolidation predictions, these aspects need to be simulated appropriately in the selected numerical approach.

---

[1] Professor of Civil Engineering, Faculty of Engineering, University of Wollongong, Wollongong City, NSW 2522, Australia

[2] PhD Students, Faculty of Engineering, University of Wollongong, Wollongong City, NSW 2522, Australia

[3] Research Fellows, Faculty of Engineering, University of Wollongong, Wollongong City, NSW 2522, Australia

[†] Correspondence to: School of Civil Engineering, Faculty of Engineering, University of Wollongong, Wollongong City, NSW 2522, Australia, e-mail: indra@uow.edu.au

INTRODUCTION

Preloading of soft clay over vertical drains is one of the most well known methods to improve the shear strength of soft soil and to reduce its post-construction settlement. Since permeability of most soft clays is very low, time required to achieve the desired settlement or shear strength can sometimes be too long to support the need for rapid construction (Johnson, 1970 and Indraratna et al., 1992). Using vertical drains, the drainage path is reduced considerably from the thickness of a soil layer to half the drain spacing in the horizontal direction (Indraratna et al., 1997). Furthermore, for most soft clay deposits, the permeability in the horizontal direction is much higher than that in the vertical direction; hence, the consolidation process can be accelerated (Jamiolkowski et al., 1983). This system has been employed effectively to improve foundation soils for railway embankments, airports and highways (Indraratna and Redana, 2000; Li and Rowe, 2002). The equivalent plane strain solution developed by the primary author and co-workers can be used as a predictive tool with acceptable accuracy. In the future the theory will be extended to include cyclic loads and cyclic pore pressures as applicable for busy rail tracks.

The performance of various types of vertical drains including sand drains, sand compaction piles, prefabricated vertical drains (geosynthetic) and gravel piles, has been studied in the past three decades. Sand drains were firstly introduced in practice around 1920's. The laboratory and field tests of the sand drain systems have been conducted initially by the California Division of Highways since the 1940's, and Kjellman (1948) introduced the prefabricated band shaped drains and cardboard wick drains for ground improvement. Typically, the prefabricated band drains consist of a plastic core with longitudinal channel wick, functioning as drain and filter jacket (fibrous material protecting the core). Basically, the dimensions of most vertical drains are in the order of 100 mm width and 4 mm thickness.

Figure 1 illustrates a typical plan of vertical drain system installation and essential instruments required to monitor the performance of soil foundation beneath an earthfill embankment. Before installing the vertical drains, general site preparations including the removal of vegetation and surficial soil, establishing site grading and

placing a compact sand blanket, are required. The sand blanket system is employed to expel water away from the drains and to provide a sound-working mat for vertical drain rigs.

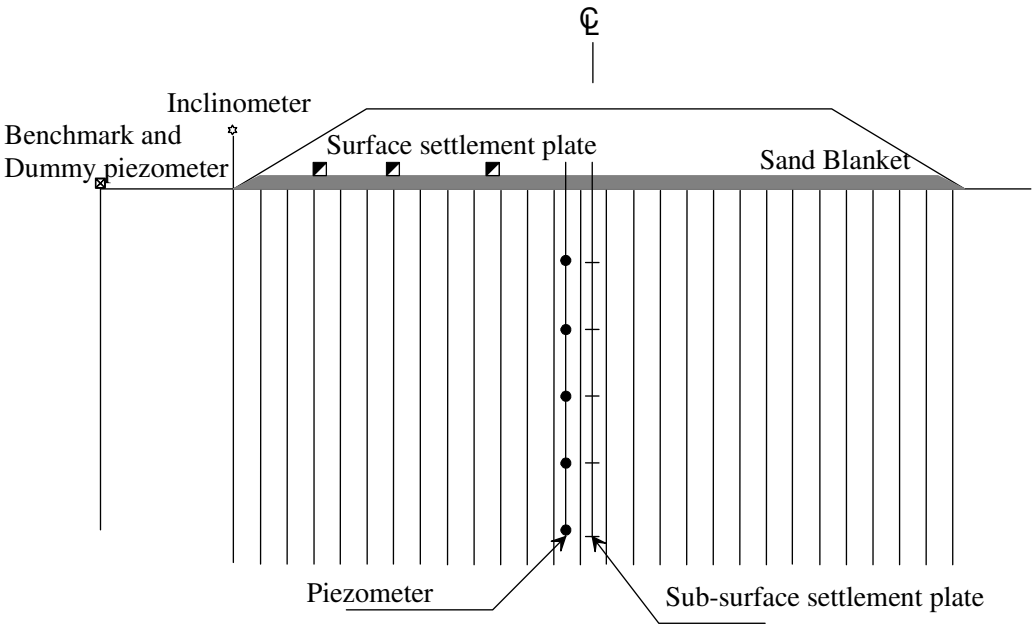

Figure 1: Vertical drain system with preloading

For a vertical drain system incorporating vacuum preloading, the installation of horizontal drains in the transverse and longitudinal directions is required after the installation of the sand blanket system (Cognon et al., 1994). Subsequently, these drains can be connected to the edge of a peripheral Bentonite slurry trench which is typically sealed with an impermeable membrane. The trenches are then filled with water to improve the sealing between the membrane and the Bentonite slurry. Finally, the vacuum pumps are connected to the prefabricated discharge module extending from the trenches. The suction head created by the pump accerelates the excess pore water pressure in the soil moving towards the drains and the surface. Figure 2 shows a typical embankment subjected to vacuum preloading.

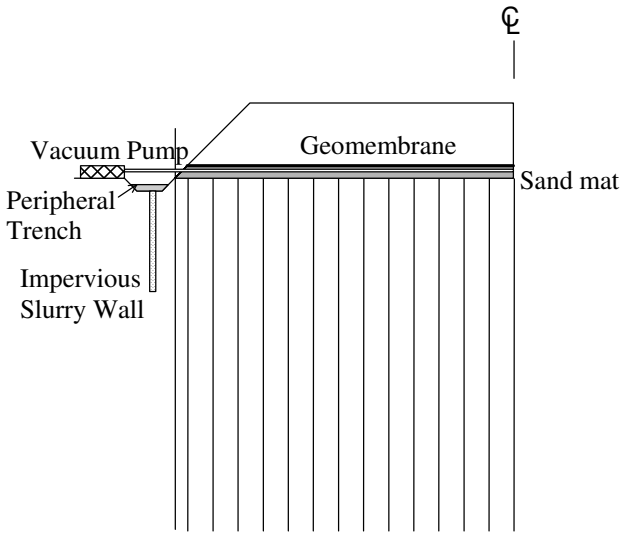

Figure 2: Vacuum preloading system

Field instrumentation for monitoring and evaluating the performance of embankments is essential to examine and control the geotechnical problems. Performance evaluation of embankements is also important to improve settlement predictions and to provide sound guidelines for future projects. Based on the construction stages, field instrumentation can be divided into two groups (Bo et al., 2003). The first group is used to prevent sudden failures during contruction (e.g. settlement plates, inclinometers and piezometers), whereas the second group is used to record changes in the rate of settlement and excess pore pressure during loading stages (e.g. multilevel settlement guages and piezometers).

DEVELOPMENT OF THE THEORY OF CONSOLIDATION WITH VERTICAL DRAINAGE

Barron (1948) presented an original comprehensive solution to the problem of radial consolidation by drain wells. He studied two extreme cases, namely, (a) free strain and (b) equal strain. Smear and well resistance effects for the case of vertical strain were considered in his solutions. Subsequently, various solutions incorporating different assumptions and boundary conditions were given in Yoshikuni and Nakanodo (1974), Holtz et al. (1991) and Hansbo (1979). Baron (1948) showed that the average consolidation obtained in both “free strain” and “equal strain” cases are nearly the same,

and the solution obtained from the "equal strain" assumption is simpler than that obtained from the "free strain" (Barron, 1948). Therefore, "equal strain" is commonly used in most radial drainage-consolidation analyses.

The average horizontal degree of consolidation, $\overline{U}_h$, of a soil cylinder with vertical drain (Figure 3) can be expressed by:

$$\overline{U}_h = 1 - exp\left(-\frac{8T_h}{\mu}\right) \tag{1}$$

and

$$\mu = ln\left(\frac{n}{s}\right) + \left(\frac{k_h}{k'_h}\right) ln(s) - 0.75 + \pi z(2l - z)\frac{k_h}{q_w}\left\{1 - \frac{k_h / k'_h - 1}{(k_h / k'_h)(n/s)^2}\right\} \tag{2}$$

where, T_h = time factor, n = ratio d_e/d_w (d_e is the diameter of equivalent soil cylinder = $2R$ and d_w is the diameter of drain = $2r_w$), s = ratio d_s/d_w (d_s is the diameter of smear zone = $2r_s$), k_h = horizontal permeability coefficient of soil in the undisturbed zone, k'_h = horizontal permeability coefficient of soil in the smear zone, z = depth, l = equivalent length of drain, which is equal to half drain length for opened end drains or entire drain length for closed end drains and q_w = well discharge capacity. A simplified form of μ can be alternatively given by:

$$\mu = ln\left(\frac{n}{s}\right) + \left(\frac{k_h}{k'_h}\right) ln(s) - 0.75 + \pi z(2l - z)\frac{k_h}{q_w} \tag{3}$$

Considering only the effect of smear, Equation 3 becomes:

$$\mu = ln\left(\frac{n}{s}\right) + \left(\frac{k_h}{k'_h}\right) ln(s) - 0.75 \tag{4}$$

Considering only the effect of well resistance, Equation 3 becomes:

$$\mu \approx ln(n) - 0.75 + \pi z(2l - z)\frac{k_h}{q_w} \tag{5}$$

For an ideal drain (i.e. smear and well resistance are ignored), the above parameter becomes:

$$\mu = \ln(n) - 0.75 \qquad (6)$$

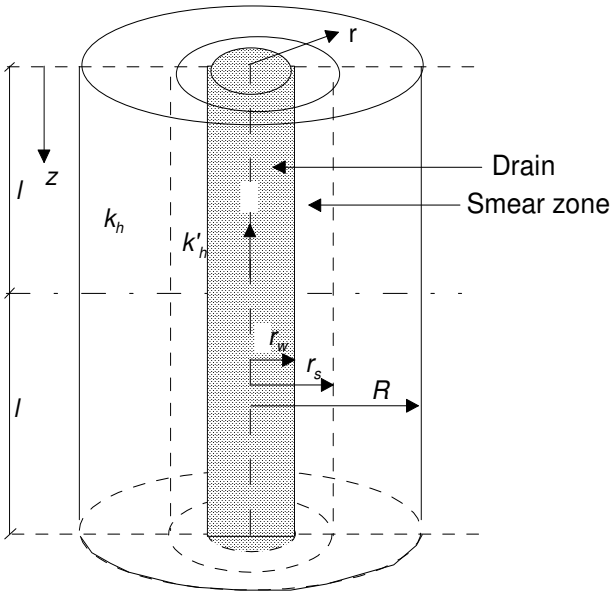

Figure 3: An axisymmetric soil cylinder with vertical drain

(adapted from Indraratna and Redana, 1997)

Recently, Indraratna and Rujikiatkamjorn (2004) introduced the analytical solutions of unit cell incorporating vacuum preloading. The large-scale laboratory results show that vacuum pressure varies along the drain length. Therefore, the efficiency of vacuum preloading is taken into account in the analytical solution by considering the vacuum pressure variation along the drain boundary (Figure 4) .

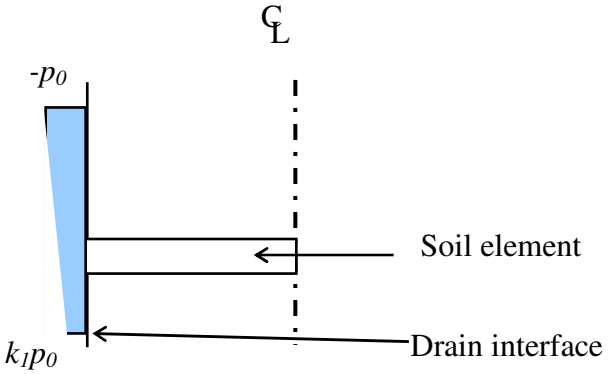

Figure 4: Vacuum pressure distribution along the drain length

Based on the above distribution (Figure 4), the analytical solution for vertical drain incorporating vacuum preloading can be given by:

$$\overline{U}_h = 1 - \left[\left(1 + \frac{p_0 G(n)}{\overline{u}_o} \right) \exp\left(-\frac{8T_h}{\mu} \right) - \frac{p_0 G(n)}{\overline{u}_0} \right] \tag{7}$$

and

$$G(n) = \frac{(1+k_1)}{2} \tag{8}$$

where, p_0 = applied vacuum pressure at the top of the drain, k_1 = ratio between vacuum pressure at the bottom of the drain and vacuum pressure at the top of the drain and $\overline{u}_0$ = initial excess pore water pressure.

Most recently, the primary author and his co-workers on an ongoing research at Wollongong University made an attempt to estimate the extent of "smear zone", caused by mandrel installation using the Cylindrical Cavity Expansion theory incorporating the modified Cam-clay model (MCC). Cavity expansion has attracted the attention of many researchers due to its numerous applications in the field of soft clay engineering. This technique is commonly employed to analyse pile driving, tunnelling and soil testing. When a mandrel is driven into soil, it will initially displace a volume of soil equal to the volume of the mandrel. A heave of soil can occur at the soil surface, up to about ten times the radius of the mandrel. At a greater depth, the soil is displaced predominantly outwards in the radial direction. Therefore, the expansion of a cylindrical cavity with a final radius equal to that of the mandrel is appropriate to predict the extent of smear zone. After the initial yielding at the cavity wall, a zone of soil extending from the cavity wall to a radial distance (r_p) will become plastic as the cavity pressure continues to increase (Figure 5). For a soil obeying the MCC model, the yielding criterion is given by:

$$\eta = \mathrm{M}\sqrt{\frac{p_c'}{p'} - 1} \tag{9}$$

where, η = stress ratio q/p' (q is the deviatoric stress $(\sigma_1-\sigma_3)/2$ and p' is the effective mean stress $(\sigma_1+2\sigma_3)/3$), M = slope of critical state line projected to q-p' plane and p'_c = effective preconsolidation pressure. The stress ratio at the elastic-plastic boundary can be found as follows:

$$\eta_p = \left(\frac{q}{p'}\right)_{r=r_p} = \frac{q_p}{p'_0} = \mathrm{M}\sqrt{OCR-1} \tag{10}$$

where, η_p = stress ratio at the elastic-plastic boundary, r = distance from central axis of the drain, $q_p = (\sigma_1-\sigma_3)/2$ at the elastic-plastic boundary and OCR is the isotropic over consolidation ratio, defined by p'_{c0}/p'_0 (p'_{c0} is the initial preconsolidation pressure and p'_0 is the initial effective mean stress). Stress ratio at any point can be determined as follows:

$$\ln\left(1-\frac{\left(a^2-a_0^2\right)}{r^2}\right) = -\frac{2(1+\nu)}{3\sqrt{3}(1-2\nu)}\frac{\kappa}{\upsilon}\eta - 2\sqrt{3}\,\frac{\kappa\Lambda}{\upsilon\mathrm{M}}\,f(\mathrm{M},\eta,OCR) \tag{11}$$

and

$$f(\mathrm{M},\eta,OCR) = \frac{1}{2}\ln\left[\frac{(\mathrm{M}+\eta)\left(1-\sqrt{OCR-1}\right)}{(\mathrm{M}-\eta)\left(1+\sqrt{OCR-1}\right)}\right] - \tan^{-1}\left(\frac{\eta}{\mathrm{M}}\right) + \tan^{-1}\left(\sqrt{OCR-1}\right) \tag{12}$$

where, a = radius of the cavity, a_0 = initial radius of the cavity, ν = Poisson's ratio, κ = slope of the overconsolidation line, υ = specific volume and $\Lambda = 1-\kappa/\lambda$ (λ is the slope of the normal consolidation line). Finally, the corresponding mean effective stress, in terms of deviatoric stress, total stress and excess pore pressure, can be expressed by the following expressions:

$$p' = p'_0\left[\frac{OCR}{1+(\eta/\mathrm{M})^2}\right]^{\Lambda} \tag{13}$$

$$q = \eta\, p' \tag{14}$$

$$p = \sigma_{rp} - \frac{q}{\sqrt{3}} + \frac{2}{\sqrt{3}}\int_r^{r_p}\frac{q}{r}dr \tag{15}$$

Employing Equations 13-15, the excess pore pressure due to mandrel driving (Δu) can be determined by:

$$\Delta u = (p - p_0) - (p' - p_0') \quad (16)$$

where, p_0 = initial total mean stress. The extent of the smear zone can be suggested as the region in which the excess pore pressure is higher than the initial overburden pressure (σ_{v0}') (Figure 5). This is because, in this region, the soil properties, such as permeability and soil anisotropy, are disturbed severely at radial distance where $\Delta u = \sigma_{v0}'$.

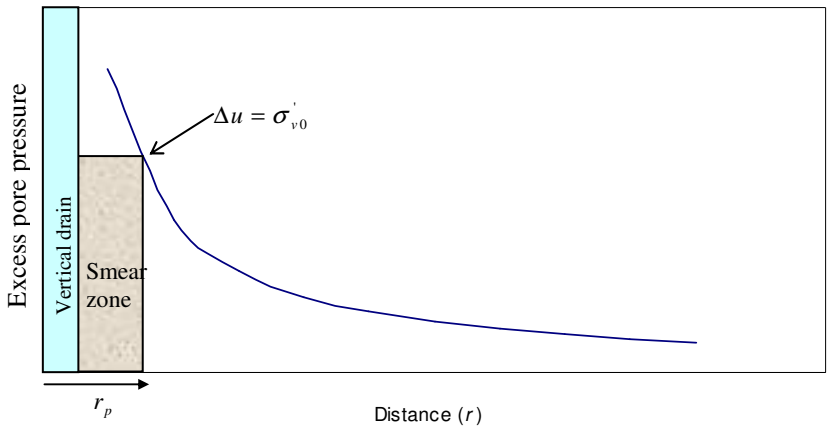

Figure 5: Smear zone prediction by the Cavity Expansion Theory

PLANE STRAIN CONSOLIDATION MODEL AND THE CONVERSION PROCEDURE

Most finite element analyses on embankments are conducted based on the plane strain assumption. However, the consolidation around vertical drains is truly axisymmetric. Therefore, to employ a realistic 2-D finite element analysis for vertical drains, the *equivalence* between the plane strain analysis and axisymmetric analysis needs to be established. Indraratna and Redana (1997) converted the vertical drain system shown in Figure 6 into an equivalent parallel drain well by adjusting the coefficient of permeability of the soil, and by assuming the plane strain cell to have a width of 2*B*. The half width of the drain b_w and half width of the smear zone b_s may be kept the same as their axisymmetric radii r_w and r_s, respectively, which gives $b_w = r_w$ and $b_s = r_s$.

Indraratna & Redana (1997) represented the average degree of consolidation in plane strain condition as follows:

$$\overline{U}_{hp} = 1 - \frac{\overline{u}}{\overline{u}_o} = 1 - exp\left(\frac{-8T_{hp}}{\mu_p}\right) \tag{17}$$

and

$$\mu_p = \left[\alpha + (\beta)\frac{k_{hp}}{k'_{hp}} + (\theta)(2lz - z^2)\right] \tag{18}$$

where, $\overline{u}_0$ = initial excess pore pressure, $\overline{u}$ = pore pressure at time t (average values) and T_{hp} = time factor in plane strain.

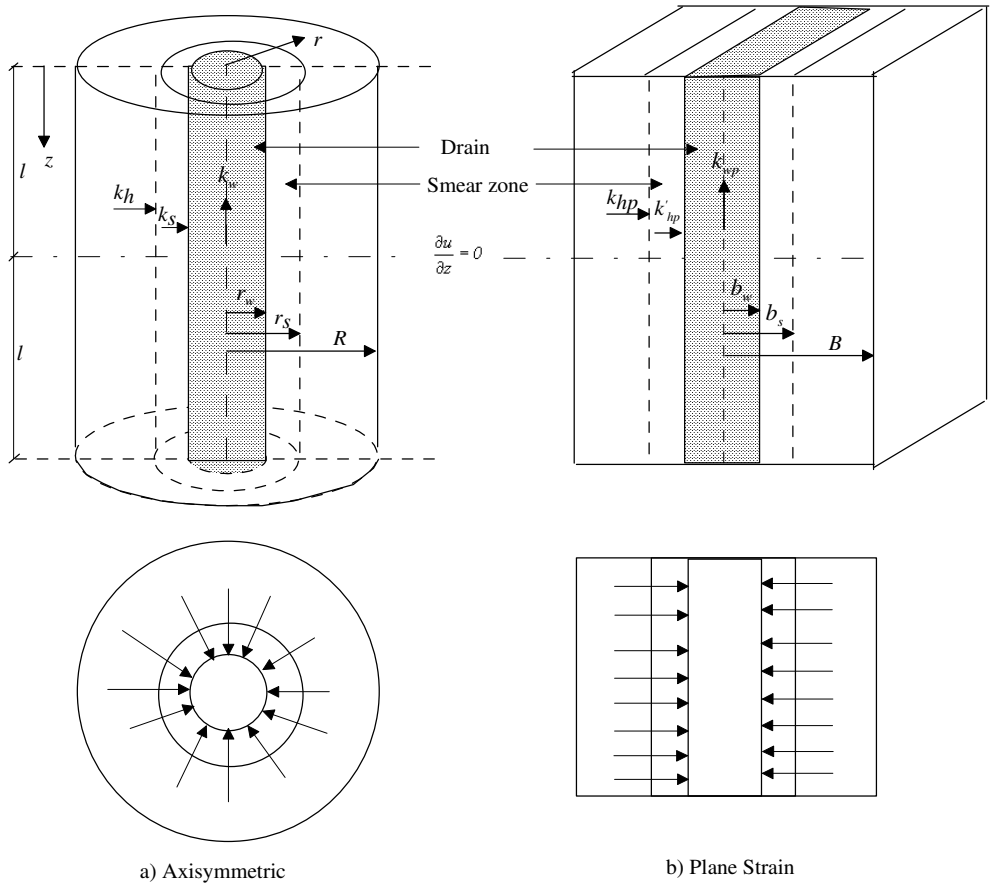

Figure 6: Conversion of an axisymmetric unit cell into plane strain condition (after Redana, 1999)

Indraratna & Rujikiatkamjorn (2004) extended the analytical solutions of unit cell incorporating vacuum preloading for the plane strain condition, as follows:

$$\frac{\bar{u}}{\bar{u}_0} = \left(1 + \frac{p_{0p}}{\bar{u}_o}\frac{(1+k_1)}{2}\right)\exp\left(-\frac{8T_{hp}}{\mu_p}\right) - \frac{p_{0p}}{\bar{u}_0}\frac{(1+k_1)}{2} \tag{19}$$

where, k_{hp} and k'_{hp} are the undisturbed horizontal and the corresponding smear zone equivalent permeabilities, respectively. The geometric parameters α, β and θ (flow term), are given by:

$$\alpha = \frac{2}{3} - \frac{2b_s}{B}\left(1 - \frac{b_s}{B} + \frac{b_s^2}{3B^2}\right) \tag{20a}$$

$$\beta = \frac{1}{B^2}\left(b_s - b_w\right)^2 + \frac{b_s}{3B^3}\left(3b_w^2 - b_s^2\right) \tag{20b}$$

$$\theta = \frac{2k_{hp}^2}{k'_{hp}q_z B}\left(1 - \frac{b_w}{B}\right) \tag{20c}$$

where, q_z = the equivalent plane strain discharge capacity.

At a given effective stress level and at each time step, the average degree of consolidation for both axisymmetric ($\overline{U}_h$) and equivalent plane strain ($\overline{U}_{hp}$) conditions are made equal, hence:

$$\overline{U}_h = \overline{U}_{hp} \tag{21}$$

Combining Equations 17 and 21 with equation 1 of original Hansbo theory (Hansbo, 1981), the time factor ratio can be represented by the following equation:

$$\frac{T_{hp}}{T_h} = \frac{k_{hp}}{k_h}\frac{R^2}{B^2} = \frac{\mu_P}{\mu} \tag{22}$$

By assuming the magnitudes of *R* and *B* to be the same, Indraratna and Redana (1997) presented a relationship between k_{hp} and k'_{hp}, as follows:

$$k_{hp} = \frac{k_h\left[\alpha+(\beta)\frac{k_{hp}}{k'_{hp}}+(\theta)\left(2lz-z^2\right)\right]}{\left[ln\left(\frac{n}{s}\right)+\left(\frac{k_h}{k'_h}\right)ln(s)-0.75+\pi\left(2lz-z^2\right)\frac{k_h}{q_w}\right]} \quad (23)$$

If well resistance is ignored in Equation 23 by omitting all terms containing *l* and *z*, the influence of smear effect can be modelled by the ratio of the smear zone permeability to the undisturbed permeability, as follows:

$$\frac{k'_{hp}}{k_{hp}} = \frac{\beta}{\frac{k_{hp}}{k_h}\left[ln\left(\frac{n}{s}\right)+\left(\frac{k_h}{k'_h}\right)ln(s)-0.75\right]-\alpha} \quad (24)$$

If smear and well resistance effects are ignored in the above expression, then the simplified ratio of plane strain to axisymmetric permeability is readily obtained, as proposed by Hird et al. (1992), as follows:

$$\frac{k_{hp}}{k_h}=\frac{0.67}{[ln(n)-0.75]} \quad (25)$$

The well resistance is derived independently and yields an equivalent plane strain discharge capacity of drains, which can be determined from the following equation:

$$q_z=\frac{2}{\pi B}q_w \quad (26)$$

For vacuum preloading, the equivalent vacuum pressure in plane strain and axisymmetric are the same.

LABORATORY TESTING USING LARGE-SCALE CONSOLIDOMETER

At the University of Wollongong, the effectiveness of prefabricated vertical drains has been extensively studied by employing large-scale laboratory consolidation tests (Figure 7). Initially, this apparatus was developed by Indraratna and Redana (1995,1998) to study the effect of smear due to vertical drain installation including sand drains and prefabricated vertical drains (PVDs). The internal diameter and the overall height of the

assembled cell are 450 mm and 1000 mm, respectively. The loading system was applied by an air jack compressor system via a piston. The settlement was measured by a Linear Variable Differential Transducer (LVDT) placed at the top of this piston. An array of strain gauge type pore pressure transducers complete with wiring to supply recommended 10 V DC supply was installed to measure the excess pore water pressures at various points. It was found that even though a larger width of the drain may cause a greater smear zone, for PVDs, the measurements and predictions indicate slightly increasing settlements due to the increased surface area, facilitating efficient pore water pressure dissipation. In contrast, for sand drains, increasing drain diameter does not necessarily improve pore pressure dissipation. In fact, a greater diameter increases the overall stiffness, especially for compacted sand or gravel, thereby decreasing surface settlement. Figure 8 shows the variation of the ratio of the horizontal to vertical permeabilities (k_h/k_v) at different consolidation pressures along the radial distance, obtained from large-scale laboratory consolidation. It can be seen that the average value of k_h/k_v starts to decrease considerably from 1.65 (outside smear zone) to 1.1 (inside smear zone). It implies that the permeability ratio between undisturbed and smear zone (k_h/k'_h) is approximately 1.5 and the extent of smear zone (r_s) is 4-5 times the radius of the vertical drain (r_w). It should be noted that k_h/k'_h ratio in the field can vary from 1.5 to 10, depending on the type of drain and installation procedures (Saye, 2003).

At present, the apparatus is further modified by applying a suction pressure at the top of the drain to study the effect of vacuum preloading. Soil unsaturation due to vertical drain installation is also further investigated by this apparatus. It is found that the vacuum pressure application accelerates the consolidation process by increasing the lateral hydraulic gradient, as shown in Figure 9. It is also found that the occurrence of soil unsaturation at the PVD boundary due to mandrel driving could retard the pore pressure dissipation in the early stage of consolidation process.

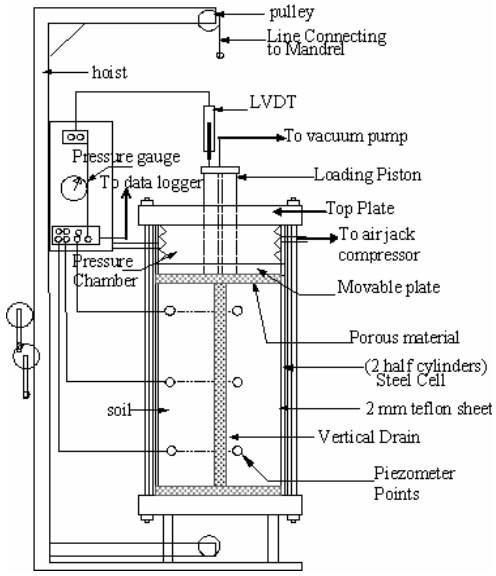

Figure 7: Schematic of large-scale consolidation apparatus (after Indraratna and Redana, 1995)

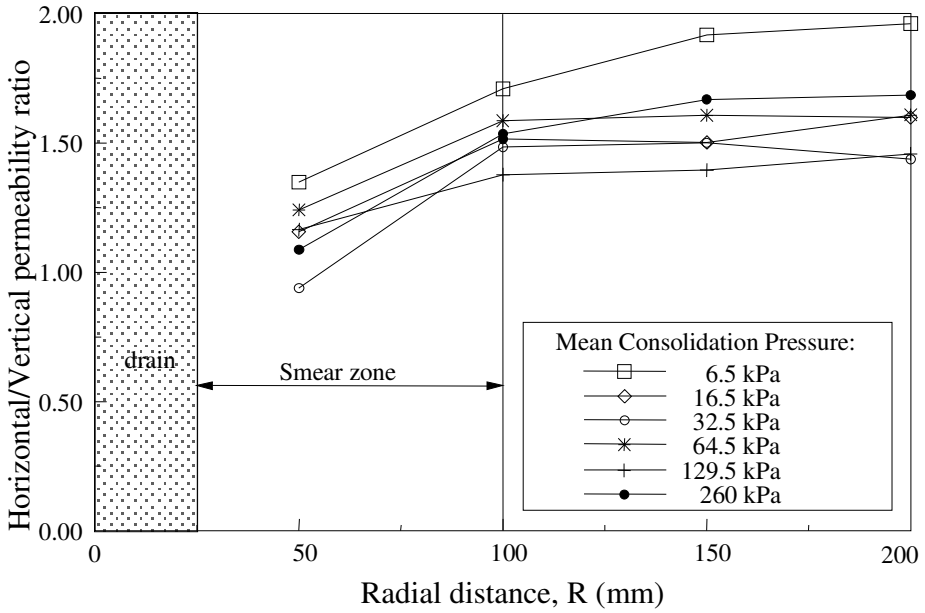

Figure 8: Ratio of k_h/k_v along the radial distance from the central drain (after Indraratna and Redana, 1995)

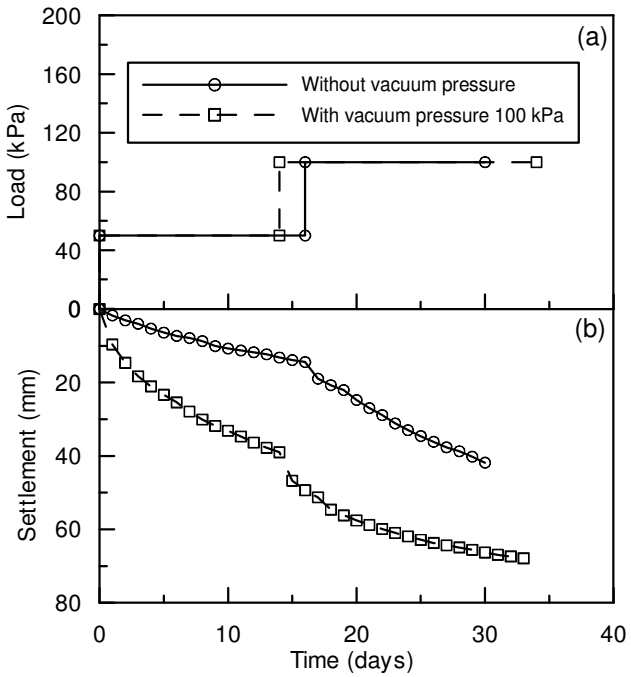

Figure 9: Soil settlement results from large-scale laboratory tests

APPLICATION OF NUMERICAL MODELLING IN PRACTICE AND FIELD OBSERVATION

Indraratna et al. (1992 and 1994) and Indraratna & Redana (2000) made an attempt to analyse the performance of two embankments constructed by the Malaysian Highway Authority at Muar plain, one built to failure with no drains, and the other with prefabricated vertical drains. At this site, soft clay foundation is mostly marine, lagoonal or deltaic origin that is characterised by high compressibility, very low permeability and low shear strength. Therefore, the ground improvement techniques are necessary to prevent excessive and differential settlements in the field. The sub-soil profiles and corresponding properties are shown in Figure 10. The subsoil is relatively uniform and consists of top weathered clay crust (2 m depth) underlain by soft to very soft silty clay layers that extend to 20 m depth. Underneath the soft clay layers, dense clayey silty sand layer can be found at 20-24 m depth. Figure 10 also illustrates the variation of water content and consolidation parameters with depth. The unit weight of soil is between 15-16 kN/m^3, except the top weathered crust, which has unit weight of 17 kN/m^3. As measured by the field shear vane, the undrained shear strength was

minimum at a depth of 3 m ($C_u \cong 8$ kPa), and this value increases linearly with depth. Extensive laboratory tests were also conducted prior to the construction of the embankments including oedometer, Unconsolidated Undrained (UU) and Consolidated Undrained (CU) triaxial tests. The performance of the two embankments constructed on the aforementioned site, is described below.

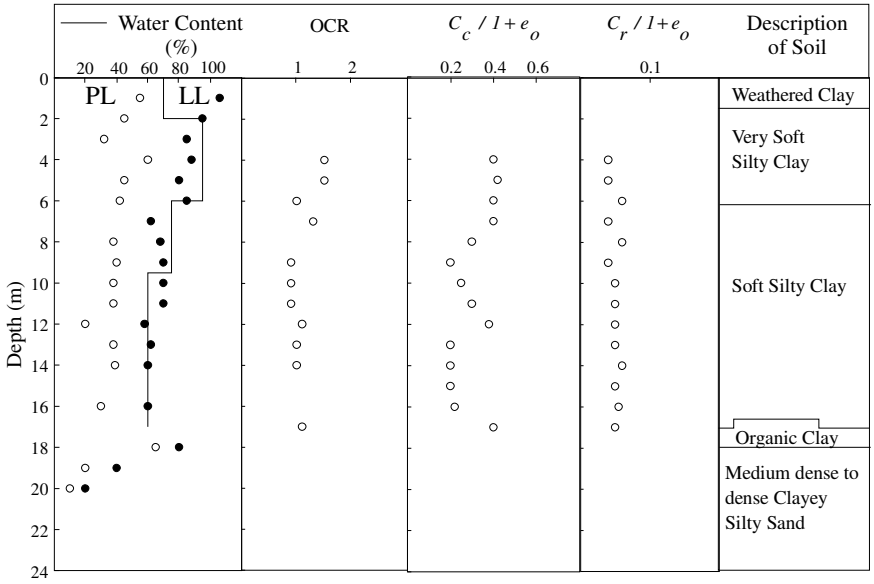

Figure 10: Variation of shear strength and consolidation parameters at Muar plain (after Redana, 1999)

PERFORMANCE OF TEST EMBANKMENT CONSTRUCTED TO FAILURE ON MUAR CLAY

One of the two test embankments at Muar plain was built to failure for the purpose of comparison with the other embankment. The failure was initiated by the development of a "quasi slip circle" type of rotational failure at a critical height of approximately 5.5 m, with a prominent tension crack propagating vertically through the crust and the fill (Figure 11). Indraratna et al. (1992) analysed the performance of the embankment using 2D finite element analysis incorporating two different constitutive soil models, namely, the Modified Cam-clay theory using the finite element program CRISP (Woods, 1992) and the hyperbolic stress-strain behaviour using the finite element code ISBILD (Ozawa

and Duncan, 1973). The modes of analysis can be divided into two types: undrained and coupled consolidation. For the undrained condition, it is assumed that the rate of loading is much *faster* than the rate of drainage. Therefore, excess pore pressures do not have adequate time to dissipate and will build up during loading and the volume change is zero. For the coupled consolidation analysis, the excess pore pressures are generated simultaneously with drainage and volume change (positive or negative) is developed. Total mean stress may also be different during loading.

Soil parameters used for the Modified Cam-clay model (MCC) in CRISP program are shown in Table 1, which also summarises the values of the bulk modulus (K_w), and the coefficient of horizontal and vertical permeabilities (k_h and k_v). A summary of soil parameters applicable for undrained and drained analyses by ISBILD is given in Table 2. The in-situ stress conditions are also incorporated in the numerical analyses and are given in Table 3. Due to insufficient expermental data, the soil properties of the topmost crust are assumed to be the same as the properties of the layer just beneath it. For the embankment surcharge (E = 5100 kPa, ν = 0.3 and γ = 20.5 kN/m^3), the shear strength parmeters, obtained from drained triaxial tests, are represented by c' = 19 kPa and ϕ' = 26^0.

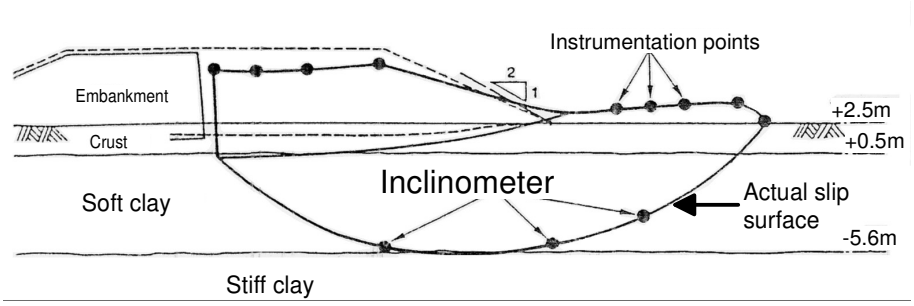

Figure 11: Failure mode of embankment and foundation (modified after Brand and Premchitt, 1989)

Table 1: Soil parameters used in the Modified Cam-clay model (CRISP)

(Source: Indraratna et al.,1992)

Depth (m)	κ	λ	M	ν	e_{cs}	$K_w \times 10^4$ (cm^2/s)	γ (kN/m^3)	$k_h \times 10^{-9}$ (m/s)	$k_v \times 10^{-9}$ (m/s)
0-2.0	0.05	0.13	1.19	0.3	3.07	4.4	16.5	1.5	0.8
2.0-8.5	0.05	0.13	1.19	0.3	3.07	1.1	15.5	1.5	0.8
8.5-18	0.08	0.11	1.07	0.3	1.61	22.7	15.5	1.1	0.6
18-22	0.10	0.10	1.04	0.3	1.55	26.6	16.1	1.1	0.6

Table 2: Soil parameters for hyperbolic stress strain model ISBILD

(Source: Indraratna et al.,1992)

Depth (m)	K	c_u (kPa)	K_{ur}	c' (kPa)	ϕ' (degree)	γ(kN/m^3)
0-2.5	350	15.4	438	8	6.5	16.5
2.5-8.5	280	13.4	350	22	13.5	15.5
8.5-18.5	354	19.5	443	16	17.0	15.5
18.5-22.5	401	25.9	502	14	21.5	16.0

Note: K and K_{ur} are modulus number and unloading-reloading modulus number used to evaluate compression and recompression behaviour of soil, respectively.

Table 3: In-situ stress conditions (Source: Indraratna et al.,1992)

Depth (m)	σ'_{vo} (kPa)	σ'_{ho} (kPa)	u (kPa)	p_c' (kPa)
0	0	0	0	110
2.5	22.0	13.2	16.7	110
8.5	56.1	23.7	75.5	40
16.5	113.1	67.9	173.6	60
22.5	135.9	81.5	212.9	60

Note: σ'_{ho}= horizontal in-situ effective stress, σ'_{vo}= vertical in-situ effective stress, u = pore water pressure.

The finite element descritisations applicable for CRISP and ISBILD are illustrated in Figures 12 and 13, respectively. The rate of embankment construction is assumed to be 0.4 m per week. At this site, various instruments were installed including piezometers, inclinometers and settlement plates (Figure 14). Excess pore pressure variations beneath the embankment, lateral and vertical displacements and mobilized shear stress contour at failure were obtained from the two finite element analyses and some of the results obtained will be descirbed below.

Figure 15 shows the comparison between the actual and predicted excess pore pressure results from CRISP at locations P2 and P7. It can be seen that the undrained analysis overpredicts the excess pore pressure, whereas the corresponding predictions from the coupled analysis are always less than those from undrained analysis and close to the field results. It is clear that the coupled consolidation analysis is more realistic, because the consolidation of the soft clay layer can be promoted during construction, due to the permeable sand deposits beneath it. Figure 15 also shows that the excess pore pressure diminishes along the lateral direction because of the decreasing effect of the surcharge.

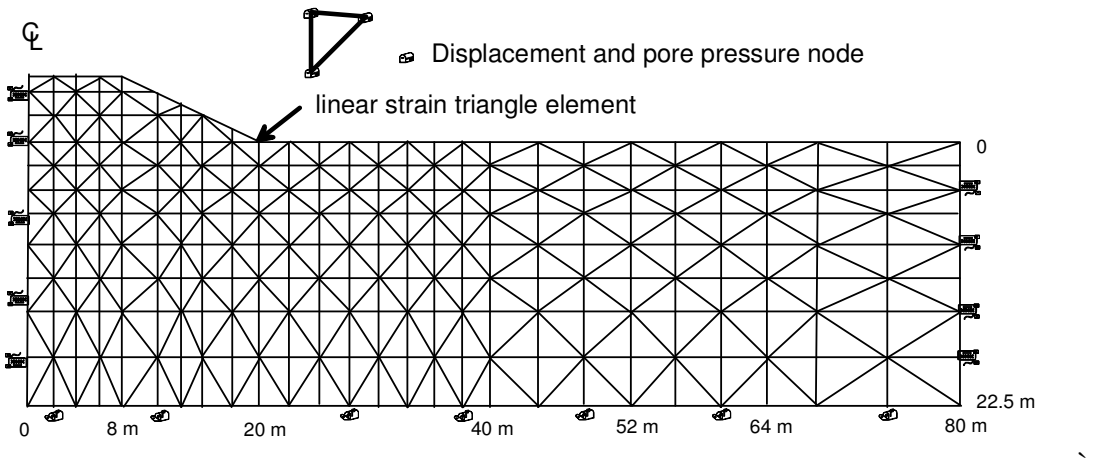

Figure 12: Finite element discretisation of embankment and subsoils for CRISP analysis (modified after Indraratna et al., 1992)

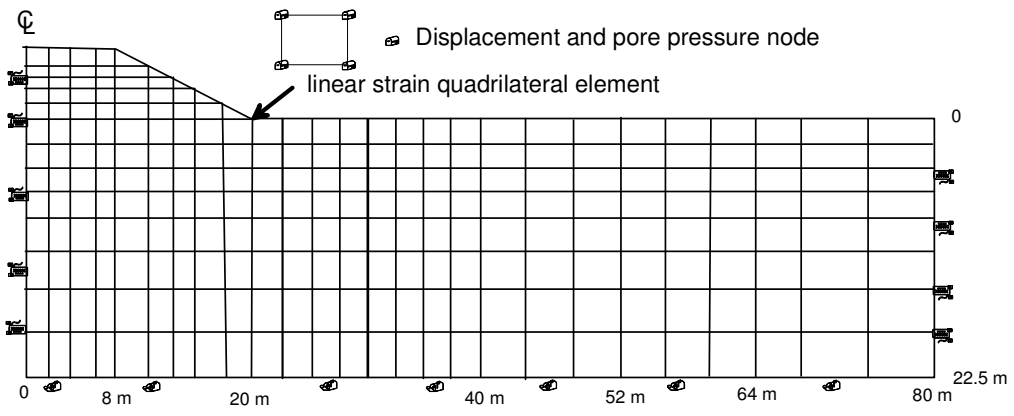

Figure 13: Finite element discretisation of embankment and subsoils for ISBILD analysis (modified after Indraratna et al., 1992)

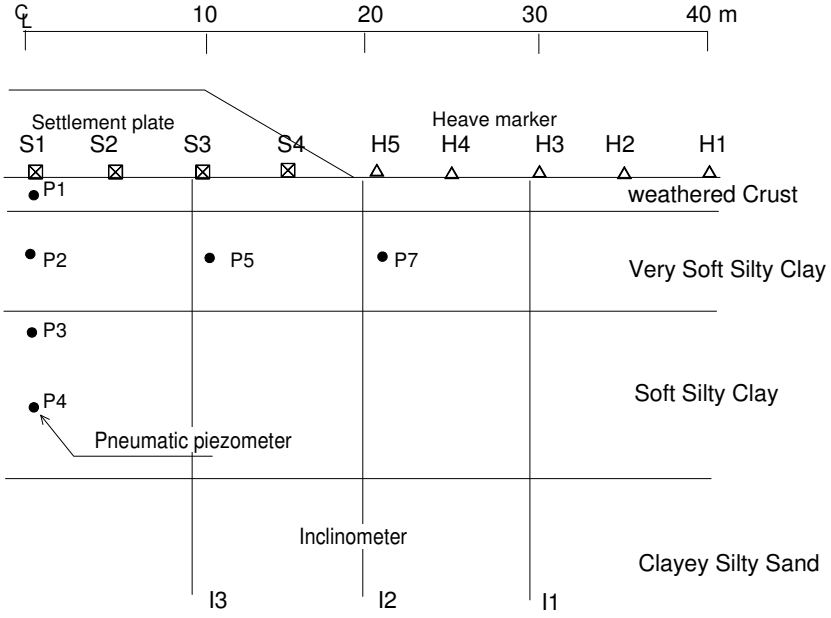

Figure 14: Cross section of Muar test embankment indicating key instruments (modified after Ratnayake, 1991)

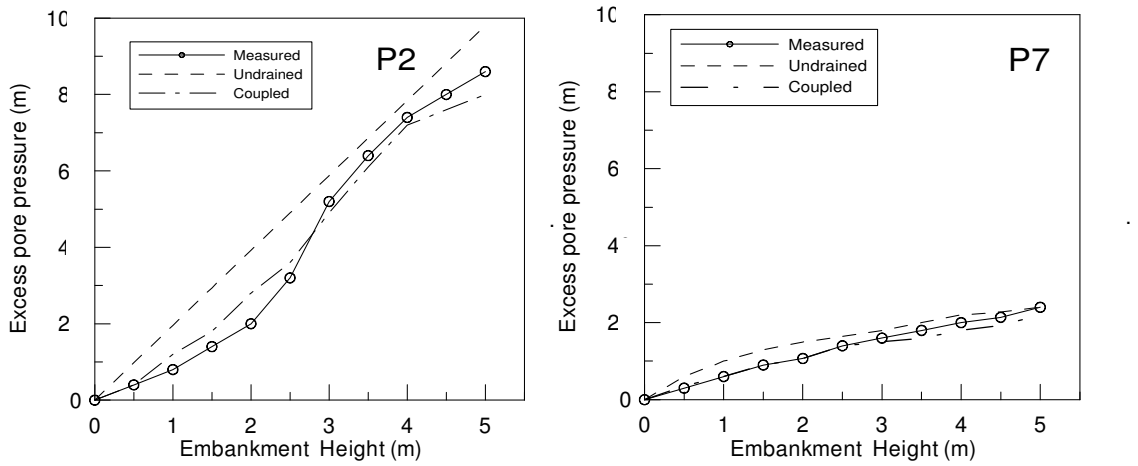

Figure 15: Variation of excess pore pressure with fill thickness (CRISP) (original data from Indraratna et al., 1992)

In Figure 16, the comparisons between the predicted and measured surface settlement for various fill heights (2-5 m) are shown. The predictions were obtained from the modified Cam-clay (CRISP) and hyperbolic (ISBILD) models At the initial fill height (less than 2 m), the undrained prediction by ISBILD agrees well with the field value, except for the area near the centreline of the embankment, whereas other predictions generally overestimate the vertical settlement. When the fill height is more than 2 m, the maximum measured vertical settlement is observed at a lateral distance 8-10 m away from the centreline, rather than at the centreline. The predictions from the coupled consolidation analysis yield better agreement with the measurements at a greater height (3-4 m, Figures 16b and 16c). At the failure height (Figure 16d), the undrained analysis using the hyperbolic stress-strain model (ISBILD) is more appropriate and gives better agreement with the field measurements.

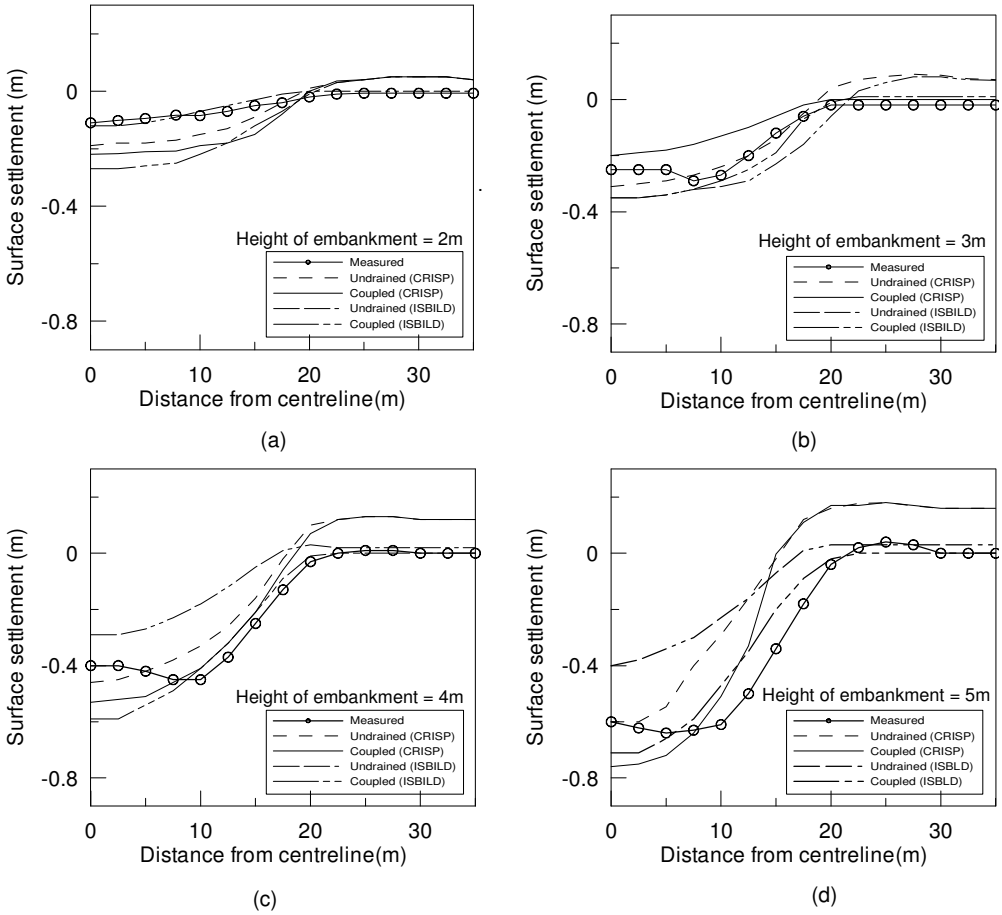

Figure 16: Surface settlement profiles for various fill heights (original data from Indraratna et al., 1992)

Figure 17 presents the variation of lateral displacements for location I3 for both the MCC model (CRISP) and the hyperbolic stress-strain model (ISBILD) at the critical height (5.5 m). As expected, the maximum lateral displacement is in the upper very soft clay layer at a depth of 5 m below the ground surface. The realistic predictions from the Modified Cam-clay can be obtained in the upper soft clay layer, whereas they deviate from the field behaviour at greater depths. The reason for this discrepency may be attributed to the accuracy of the soil parameters used and the simulation of plane strain condition.

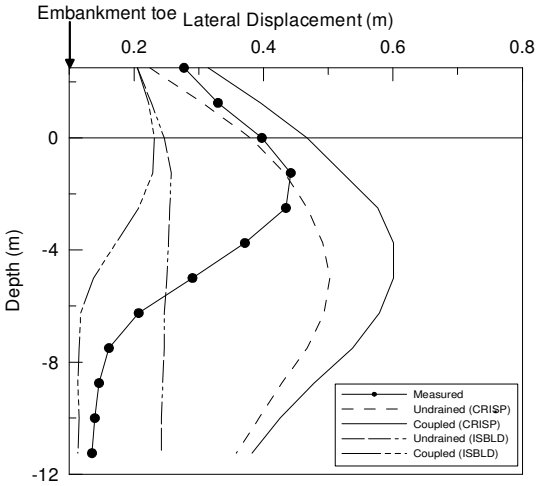

Figure 17: Lateral displacement profile at failure
(modified after Indraratna et al., 1992)

The zones of yielding and potential failure surface are interpreted based on the boundaries of yielded zone and maximum displacement vectors using the coupled consolidation from CRISP. The predicted shear band based on the maximum incremental displacement is shown in Figure 18. The boundaries of yielded zone approaching the critical state are shown in Figure 19, where each contour indicates the current field height. The yielded zone can be found close to the bottom of the soft clay layer and subsequently develops to the centreline of the embankement. It verifies that the actual failure surface is within the predicted shear band.

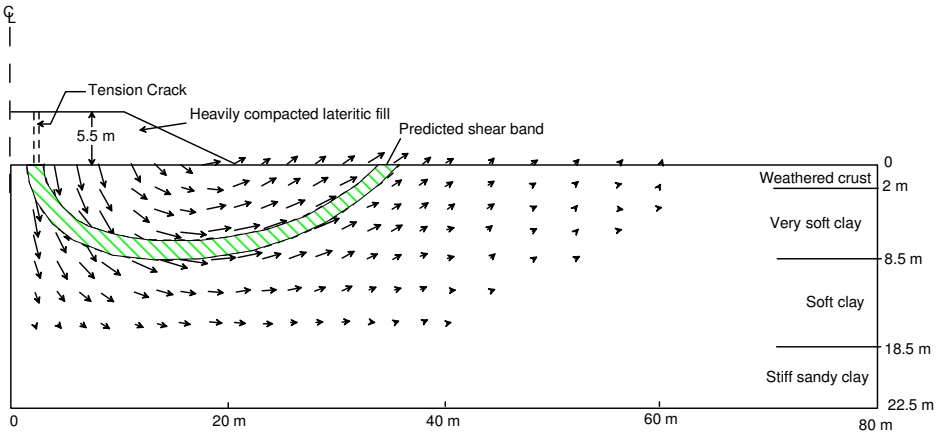

Figure 18: Maximum incremental development of failure
(modified after Indraratna et al., 1992)

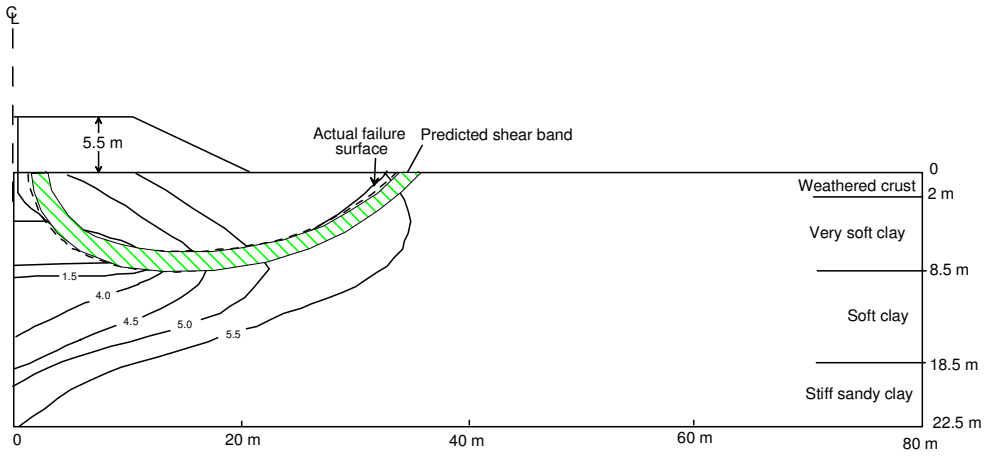

Figure 19: Boundary zones approaching critical state with increasing fill thickness (CRISP) (modified after Indraratna et al., 1992)

PERFORMANCE OF TEST EMBANKMENT STABILISED WITH VERTICAL DRAINS ON SOFT CLAY

Indraratna et al. (1994) and Indraratna & Redana (2000) investigated the effect of ground improvement by preloading over vertical drains at a site located on the Muar plain, Malaysia. The plane strain analysis incorporating the MCC model considering only the coupled consolidation analysis was employed in the finite element code CRISP. Figure 20 shows the cross section of the embankment, together with the subsoil profile and PVDs installed in a triangular pattern at spacing of 1.3 m. In this analysis, the soil foundation was descritised using linear strain quadrilateral (LSQ) elements (Figure 21). The vertical drains were modelled by using a relatively fine mesh to prevent unfavourable aspect ratio of the mesh.

Table 4 gives details of the drain parmeters and Table 5 summarises the Cam-clay parameters for Muar clay subsoils used in CRISP. The relevent soil properties were obtained from CU triaxial tests (Ratnayake, 1991). Based on the matching procedure, expalined earlier and proposed by Indraratna and Redana (1995), the measured horizontal and vertical permeabilies at the in-situ soil condition, and the equivalent calculated plane strain values, are shown in Table 6 (Equations 23-25).

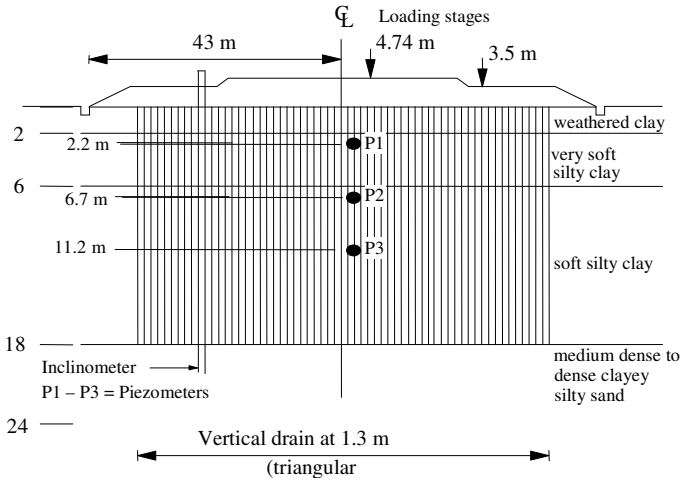

Figure 20: Cross section of embankment with soil profile at Muar clay, Malaysia (Indraratna and Redana, 2000)

Table 4: Vertical drain parameters of the vertical drain system of Muar embankment

Vertical drain parameter	Value
Spacing, d (m)	1.3
Equivalent drain spacing, d_e (m)	1.365
Length (m)	18
Equivalent drain diameter, d_w (m)	0.07
s = d_s/d_w	5.7

Table 5: Modified Cam-clay parameters used in CRISP (Source: Indraratna and Redana, 2000)

Depth (m)	λ^*	κ	e_{cs}	M	ν	γ(kN/m^3)
0-2.0	0.30	0.06	3.10	1.19	0.29	16.5
2.0-5.5	0.60	0.06	3.06	1.19	0.31	15.0
5.5-8.0	0.30	0.05	3.06	1.12	0.29	15.5
8.0-18.0	0.35	0.035	1.61	1.07	0.26	16.0

Note: * The values of λ tabulated are for Stage 2 loading. At Stage 1 of construction due to the lower applied load λ values were taken to be λ_{oc} = 0.16.

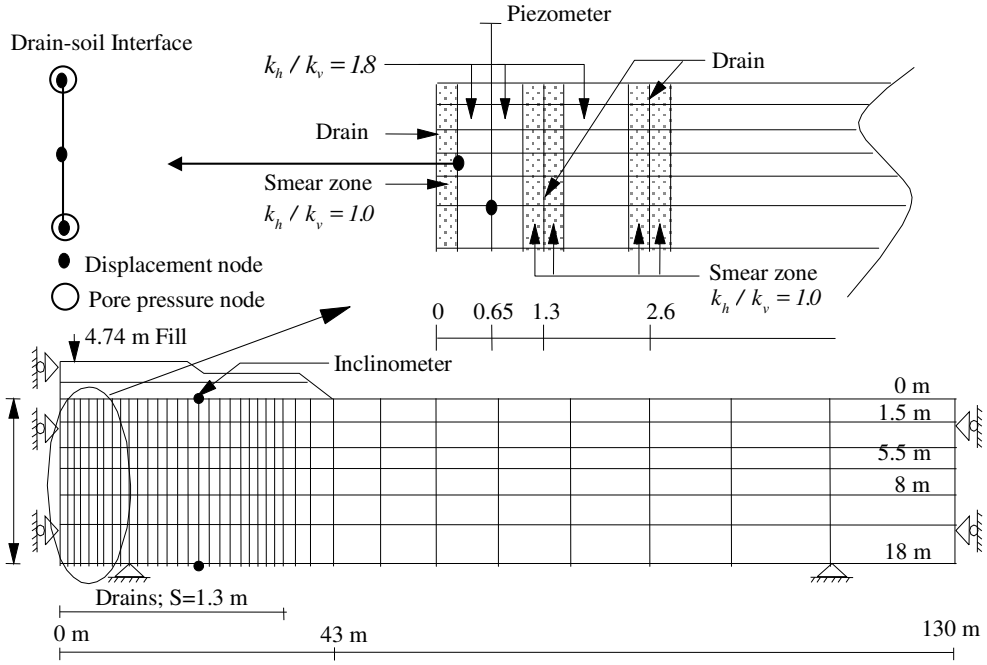

Figure 21: Finite element mesh descretisation of the embankment for plane strain analysis, Muar clay, Malaysia (Indraratna and Redana, 2000)

Table 6: Permebility coefficients used in the finite element analysis (Source: Indraratna and Redana, 2000)

Depth (m)	$k_h \times 10^{-9}$ (m/s)	$k_v \times 10^{-9}$ (m/s)	$k_{hp} \times 10^{-9}$ (m/s)	$k'_{hp} \times 10^{-9}$ (m/s)
0-2.0	6.4	3.0	1.9	1.7
2.0-5.5	5.2	2.7	1.6	1.6
5.5-8.0	3.1	1.4	9.5	7.9
8.0-18.0	1.3	0.6	3.9	3.4

The embankment load was applied in two stages. During Stage 1 of construction, the embankment was raised to a height of 2.57 m in 14 days. After rest period of 105 days, additional fill compacted to unit weight of 20.5 kN/m^3 was placed (Stage 2), until the embankment reached a height of 4.74 m in 24 days. The settlements and excess pore water pressures at the centreline were monitored for more than a year.

The comparisons between the actual and predicted settlements at the ground surface and at a depth of 5.5 m, are shown in Figure 22. It can be seen that, for the surface settlement, the predicted results with smear effect and well resistance quite agree well with the measured value (Figure 22a). It can also be seen that the inclusion of smear effect gives more accurate predictions. At 5.5 m depth, the predictions including the smear effect and well resistance, underestimate slightly the settlements beyond 200 days, while the results based on "no smear" condition overpredict the settlements (Figure 22b). The predicted and measured excess pore water pressures at the centreline and a depth of 11.2 m are shown in Figure 23. It can be noticed that the inclusion of smear zone predicts accurately the excess pore pressure up to Stage 2, whereas the inclusion of well resistance does not lead to significant improvement. This implies that the well resistance is less important for these PVDs than the smear effect. As expected, the perfect drain predictions underestimate the actual excess pore pressures.

An inclinometer was installed at 23 m away from the centreline of the embankment. The measured and predicted lateral displacements at 294 days after the beginning of the embankment construction are shown in Figure 24. It can be seen that the predicted lateral displacements agree well with the measured values when the effects of both smear and well resistance were included.

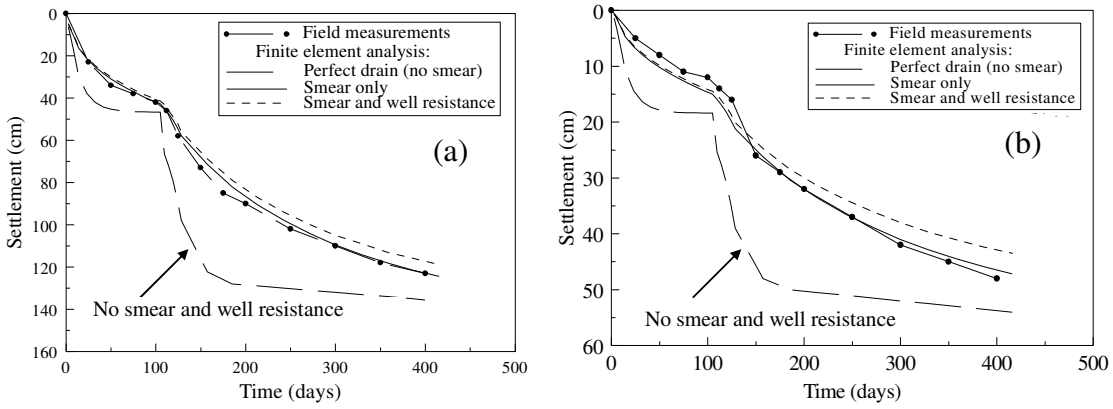

Figure 22: Total settlements at: (a) Ground surface and (b) a depth of 5.5 m below ground level, along embankment centreline, Muar clay (modified after Indraratna and Redana, 2000)

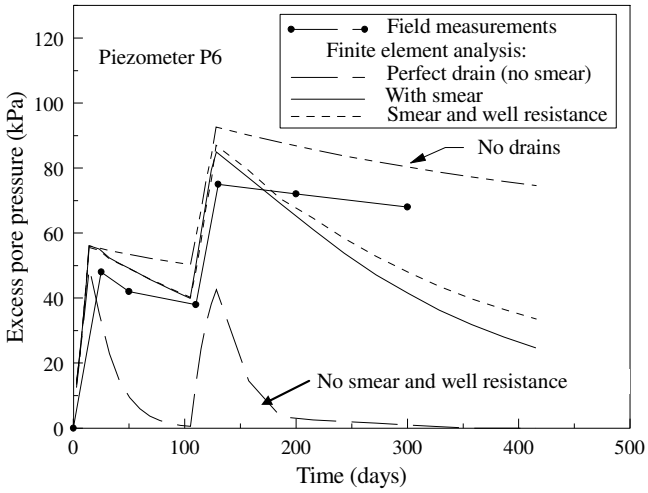

Figure 23: Variation of excess pore water pressures at embankment centreline for piezometer P6 at 11.2 m below the ground level (Indraratna and Redana, 2000)

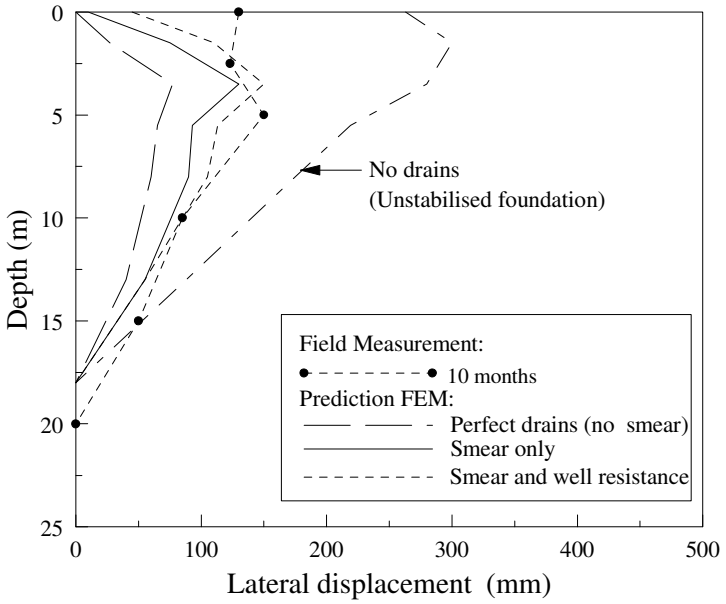

Figure 24: Lateral displacement profiles at 23 m away from centreline of embankments after 294 days (Indraratna and Redana, 2000)

The performance of the embankments stabilised with and without vertical drains was compared based on normalised deformation, as shown in Table 7. The ratios of the maximum lateral displacement to fill height (β_1) and the maximum settlement to fill

height (β_2) were considered as stability indicators. In comparison with the unstabilised embankment constructed to failure discussed earlier (Indraratna et al., 1992), the stabilised foundation is characterised by considerably smaller values of β_1, highlighting the obvious implication on stability. The normalised settlement (β_2) on its own does not seem to be a convincing indicator of instability.

Table 7: Effect of ground improvement on normalised deformation factors (Indraratna et al., 1997)

Ground improvement scheme	β_1	β_2
Embankment rapidly constructed to failure on untreated foundation (h = 5.5m)	0.104	0.164
Prefabricated vertical band drains in triangular pattern at 1.3 m spacing (h = 4.75 m)	0.034	0.274

CONCLUSIONS

Preloading techniques with vertical drains have been used widely to reduce post construction settlement and to accelerate the consolidation process in thick soft soil deposits. However, soil unsaturation at the vertical drain boundary due to mandrel driving could delay the excess pore pressure dissipation in the early stage of consolidation process. In addition, the rate of settlements and pore pressures dissipation associated with vertical drains are difficult to predict accurately. This difficulty may be attributed to the complexity of evaluating the correct magnitudes of soil parameters inside and outside the smear zone as well as the unsaturation zone at the soil-drain interface. Therefore, it is crucial to use appropriate laboratory techniques to measure these parameters, preferably employing the realistic stress paths. Using a large-scale consolidometer, it was found that the smear zone radius is 4-5 times the radius of the vertical drain and the soil permeability in the smear zone is higher than that in the undisturbed zone by 1.5-2 times.

Numerical finite element methods have been increasingly employed to predict soil consolidation behaviour. In the field, where many PVDs are installed, true 3D finite

element analysis is difficult and the equivalent 2D plane strain FEM analysis is most convenient given the computational efficiency. However, the classical axisymmetric solutions cannot be used directly in any plane strain finite element analysis without reasonable simplification. Therefore, the development of equivalent plane strain model that can provide good match with the measured data is necessary. In addition, the accurate predictions of settlements, excess pore water pressures dissipations and lateral movements involve careful evaluation of soil parameters associated with actual stress path during loading stages. In this study, the performance of soft clay subjected to preloading was predicted confidently by the coupled consolidation model in 2D FEM. The prediction from the undrained analysis gave unreliable results except at the centreline of the embankment. The finite element analysis also displayed that the correct mode of failure by considering the incremental displacement vectors and mobilised shear stress contours, can be predicted. It was revealed that the inclusion of smear effect is more important in predicting the settlements than the well resistance. Based on the normalised deformation analysis, foundations stabilised by the PVDs minimises lateral movement, thereby increasing the stability of the foundations.

ACKNOWLEDGEMENTS

The authors wish to thank the CRC for Railway Engineering and Technologies (Australia) for its continuous support and the Malaysian Highway Authority for providing the trial embankments data. The authors also express their appreciation to David Christie (RailCorp, Sydney) for his continuous assistance and advice. In addition, assistance of Prof. A.S. Balasubramaniam (formerly at Asian Institute of Technology, Bangkok, Thailand) is gratefully appreciated. A number of past research students of Prof. Indraratna, namely, Balachandran, Ratnayake, Redana and Bamunawita have also contributed to the contents of this keynote paper through their research work.

REFERENCES

Barron, R.A. 1948. Consolidation of fine-grained soils by drain wells. Transactions ASCE, Vol. 113, pp. 718-724.

Bo, M.W., Chu, J., Low, B.K. and Choa, V. 2003. Soil improvement; prefabricated vertical drain techniques. Thomson Learning, Singapore.

Brand, E.W. and Premchitt, J. 1989. Moderator's report for the predicted performance of the Muar test embankment. Proc. International Symposium on Trial Embankment on Malysian Marine Clays, Kuala Lumpur, Malaysia, Vol. 2, pp. 1/32-1/49.

Cognon, J.M., Juran, I. and Thevanayagam, S. 1994. Vacuum consolidation technology-principles and field experience. Proc. Conference on Foundations and Embankments Deformations, College Station, Texas, Vol. 2, pp.1237-1248.

Hansbo, S. 1979. Consolidation of clay by band-shaped prefabricated drains. Ground Engineering, Vol. 12, No. 5, pp. 16-25.

Hansbo, S. 1981. Consolidation of fine-grained soils by prefabricated drains. Proc. 10th Int. Conf. of Soil Mech. and Found. Eng., Stockholm, Vol. 3, pp. 677-682.

Hird, C.C., Pyrah, I.C., and Russell, D. 1992. Finite element modelling of vertical drains beneath embankments on soft ground. Geotechnique, Vol. 42, No. 3, pp. 499-511.

Holtz, R.D., Jamiolkowski, M., Lancellotta, R. and Pedroni, S. 1991. Prefabricated vertical drains: design and performance. CIRIA Ground Engineering Report: Ground Improvement, Butterworth-Heinemann Ltd, UK, 131 p.

Indraratna, B., Balasubramaniam, A. S. and Balachandran, S. 1992. Performance of test embankment constructed to failure on soft marine clay. Journal of Geotechnical Engineering, ASCE, Vol. 118, No. 1, pp. 12-33.

Indraratna, B., Balasubramaniam, A. S. and Ratnayake, P. 1994. Performance of embankment stabilized with vertical drains on soft clay. Journal of Geotechnical Engineering, ASCE, Vol. 120, No. 2, pp. 257-273.

Indraratna, B., Balasubramaniam, A. S. and Sivaneswaran, N. 1997. Analysis of settlement and lateral deformation of soft clay foundation beneath two full-scale embankments. International Journal for Numerical and Analytical Methods in Geomechanics, Vol. 21, pp. 599-618.

Indraratna, B., Bamunawita, C., Redana, I. W. and McIntosh, G. 2002. Keynote paper: Modelling of prefabricated vertical drains in soft clay and evaluation of their effectiveness in practice. Proc. 4th Int. Conf. on Ground Improvement Techniques, Malaysia, pp. 47-62.

Indraratna, B. and Redana, I. W. 1995. Large-scale radial drainage consolidometer with central drain facility. Australian Geomechanics, Vol. 29, pp. 103-105.

Indraratna, B. and Redana, I. W. 1997. Plane strain modelling of smear effects associated with vertical drains. Journal of Geotechnical Engineering, ASCE, Vol. 123, No. 5, pp. 474-478.

Indraratna, B. and Redana, I. W. 1998. Laboratory determination of smear zone due to vertical drain installation. Journal of Geotechnical and Geoenvironmental Engineering, ASCE, Vol. 124, No. 2, pp. 180-184.

Indraratna, B. and Redana, I W. 1999. Closure: Plane strain modelling of smear effects associated with vertical drains. Journal of Geotechnical Engineering, ASCE, Vol. 123, No. 5, pp. 474-478.

Indraratna, B. and Redana, I W. 2000. Numerical modelling of vertical drains with smear and well resistance installed in soft clay. Canadian Geotechnical Journal, 37, pp. 132-145.

Indraratna, B. and Rujikiatkamjorn, C. 2004. Mathematical modelling and field evaluation of embankment stabilized with vertical drains incorporating vacuum preloading. Proc. 5th International Conference on Case Histories in Geotechnical Engineering, pp. 2.05/1-2.05/8.

Jamiolkowski, M., Lancellotta, R. and Wolski, W. 1983. Precompression and speeding up consolidation. Proc. 8th ECSMFE, Vol. 3, pp. 1201-1206.

Johnson, S.J. 1970. Precompression for improving foundation soils. J. Soil. Mech. Found. Div., ASCE, Vol. 96, No. 1, pp. 111-114.

Kjellman, W. 1948. Accelerating consolidation of fine grain soils by means of cardboard wicks. Proc. 2nd ICSMFE, Vol. 2, pp. 302-305.

Li, A.L. and Rowe, R.K. 2002. Combined effect of reinforcement and prefabricated vertical drains on embankment performance. Canadian Geotechnical Journal, Vol. 38, pp. 1266-1282.

Ozawa, Y. and Duncan, J.M. 1973. ISBILD: A computer program for static analysis of static stresses and movement in embankment. University of California, Berkeley, Calif.

Ratnayake, A.M.P. 1991. Performance of test embankments with and without vertical drains at Muar flats site, Malaysia. Master Thesis, GT90-6, Asian Institute of Technology, Bangkok.

Redana, I.W. 1999. Effectiveness of vertical drains in soft clay with special reference to smear effect. PhD Thesis, University of Wollongong, NSW, Australia.

Saye, S.R. 2003. Assessment of soil disturbance by the installation of displacement sand drains and prefabricated vertical drains. Geotechnical Special Publication No. 119, ASCE, pp. 325-362.

Shang, J.Q., Tang, M. and Miao, Z. 1998. Vacuum preloading consolidation of reclaimed land: a case study, Canadian Geotechnical Journal, Vol. 35, pp.740-749.

Woods, R. 1992. SAGE CRISP technical reference manual. The CRISP Consortium Ltd. UK.

Yoshikuni, H. and Nakanodo, H. 1974. Consolidation of fine-grained soils by drain wells with finite permeability. Japan Society Soil Mechanics and Foundation Engineering, Vol. 14, No. 2, pp. 35-46.